Spin fluctuation, thermal expansion anomaly, and pressure effects on the Néel temperature of β-MnM (M=Ru, Os, and Ir) alloys

M. Miyakawa, R. Y. Umetsu, M. Ohta, and A. Fujita
Department of Materials Science, Graduate School of Engineering, Tohoku University, Aoba-yama 02, Sendai 980-8579, Japan

K. Fukamichi
Institute of Multidisciplinary Research for Advanced Materials, Tohoku University, Sendai, 980-8577, Japan and Department of Materials Science, Graduate School of Engineering, Tohoku University, Aoba-yama 02, Sendai 980-8579, Japan

T. Hori
Shibaura Institute of Technology, Saitama-city, Saitama 330-8570, Japan
(Received 8 October 2004; revised manuscript received 12 May 2005; published 16 August 2005)

The specific heat and the thermal expansion under ambient pressure and the temperature dependence of magnetic susceptibility under applied pressure have been investigated for β-$Mn_{1-x}M_x$ (M=Ru, Os, and Ir) alloys by taking spin fluctuations into consideration. From powder neutron diffractions for β-$Mn_{0.75}Os_{0.25}$ alloys, the magnetic Bragg peaks was observed at 10 K, which is the first direct confirmation of a long-range magnetic order in β-Mn alloys. The relationship between the pressure dependence of the Néel temperature dT_N/dP and T_N is explained by the Ehrenfest equation. A significantly large thermal expansion coefficient in a wide range of temperature above T_N is clearly correlated with spin fluctuations. At low and finite temperatures, the effects of spin fluctuations as a function of the Néel temperature in both the weak itinerant-electron antiferromagnetic state and intermediate antiferromagnetic state are common to β-Mn alloys, regardless of the kinds of additional elements.

DOI: 10.1103/PhysRevB.72.054420 PACS number(s): 75.50.Ee, 75.40.Cx

I. INTRODUCTION

β-Mn has no long-range magnetic ordering down to the lowest temperatures,[1–3] exhibiting significant spin fluctuation effects such as a large electronic specific heat coefficient.[4,5] In addition, the value of the nuclear spin lattice relaxation rate $1/T_1$ follows a $T^{1/2}$ dependence, which has been explained within the framework of the self-consistent renormalization (SCR) theory for nearly and weak itinerant-electron antiferromagnets, implying that spin fluctuations are reflected in antiferromagnetic correlations even in the paramagnetic state.[6,7]

In β-Mn structure ($P4_132$), the 20 Mn sites in the cubic unit are divided into two kinds of Mn sites, that is, site 1 (8c) and site 2 (12d).[8,9] The value of $1/T_1$ of Mn at site 2 is about 20 times larger than that of Mn at site 1, implying that Mn at site 2 is more magnetic.[1,10] Accordingly, the magnetic properties of the β-Mn alloys are affected by the difference in the Mn site. β-MnFe, β-MnCo, and β-MnNi (Ref. 11) alloy systems, in which almost all additional atoms occupy site 1, have been regarded as antiferromagnets because the value of $1/T_1$ in the β-Mn alloys with a small amount of additional element follows a $T^{1/2}$ dependence and the broadening of the NMR spectra ascribed to the magnetic ordering.[7,12,13] The stabilization of the antiferromagnetic ordering has been attributed to the increase of the lattice constant and the d-electron number.[12,13] Large values of the electronic specific heat coefficient have been discussed by using the spin fluctuation theory.[14]

β-MnAl alloy systems, in which the additional elements dominantly occupy at site 2, were extensively studied in the last decade, and it was suggested that the magnetic state changes from a spin-liquid state to a spin-glass-like state with increasing Al concentrations.[15–20] It has been pointed out that site 2 sublattices can be regarded as geometrical triangular lattices, resulting in a highly frustrated magnetic state, which is one of the reasons why β-Mn has no magnetic ordering, though the antiferromagnetic correlation between the Mn moments is clearly present.[16,17] Several band calculations have been performed for β-Mn.[21–24] It should be noted that the magnetic properties of β-Mn are remarkably different, depending on the calculation conditions. For example, it has been pointed out that the antiferromagnetic coupling between site 1 and site 2 is strongest in a slightly expanded state, leading to the stabilization of a ferrimagnetic phase.[24]

More recently, on the other hand, several kinds of β-Mn alloy systems, where the additional elements mainly occupy Mn Site 1, have been reported. We have investigated the platinum group elements such as Ru, Os, and Ir, which are almost substituted at site 1 in β-Mn.[25–29] From the temperature dependence of magnetic susceptibility, the Néel temperature T_N has been defined as the peak or inflection point. Antiferromagnetic properties of itinerant-electron systems like β-MnRu,[25] β-MnOs,[26–28] and β-MnIr (Ref. 29) alloys have been explained by considering spin fluctuations.[30] The maximum of the Néel temperature in the β-$Mn_{1-x}Os_x$ alloys extends to about 200 K, which is about twice as large as that in the other β-Mn alloys.[26] However, strictly speaking, the long-range antiferromagnetic ordered state of these alloys should be directly verified because pure β-Mn metal is an

enhanced Pauli paramagnet with a strong antiferromagnetic correlation and the magnetic properties of β-Mn alloys are expected to be complicated as mentioned above. Until recent years, there are no reports on the direct confirmation of the antiferromagnetic state of β-Mn alloys.[31–33] Very recently, from powder neutron diffractions, we have demonstrated that β-$Mn_{0.75}Os_{0.25}$ alloys have a long-range antiferromagnetic order. Accordingly, we can regard the peak or the inflection point in the susceptibility curves as the Néel temperature for several kinds of β-MnRu, β-MnOs, and β-MnIr alloys.

To clarify the change in the magnetic state with the composition for the β-$Mn_{1-x}M_x$ (M=Ru, Os, and Ir) alloy systems, it is meaningful to investigate the specific heat and thermal expansion characteristics closely related to spin fluctuations. By using the magnetic data under applied pressures, the pressure dependence of the Néel temperature is discussed in connection with the magnetovolume effects and the change of the magnetic state. The variation of the thermal expansion coefficient with the composition is discussed in terms of spin fluctuations and connected with the variation of the electronic specific heat coefficient.

II. EXPERIMENTS

The alloying was carried out by arc melting. The specimens were quenched into ice water from 1273 K after annealing for 2 h. No extra phase was detected by x-ray powder diffraction measurements with Cu Kα radiation. The alloy compositions were determined by an energy dispersive x-ray spectroscopy (EDXS).

The powder neutron diffraction experiments were carried out with a multicounter-type diffractometer, HERMES (Ref. 34) of Institute for Materials Research, Tohoku University, installed in the JRR-3M reactor of the Japan Energy Research Institute. The wavelength was 1.820 35 Å. The diffraction patterns were obtained in the 2θ range from 3° to 152° in a step of 0.1°. The temperature dependence of magnetic susceptibility under zero-field cool and 0.1 T was measured with a superconducting quantum interference device (SQUID) magnetometer, applying up to 0.7 GPa by using a piston-cylinder cell made of a Cu-Ti alloy.[35]

The specific heat measurement was carried out by a relaxation method. The thermal expansion curves were obtained with a differential transformer-type dilatometer and also a three-terminal capacitance. Mössbauer spectra of β-$Mn_{0.99-x}Os_xFe_{0.01}$ alloys containing enriched ^{57}Fe were obtained with a constant acceleration-type spectrometer utilized a ^{57}Co-Rh source, calibrating with α-Fe foil.

III. RESULTS AND DISCUSSION

Figure 1 shows the powder neutron diffraction patterns of β-$Mn_{0.75}Os_{0.25}$ alloys at 10 and 295 K, together with the calculated pattern of the nuclear diffractions from the (110), (111), (210), and (211) planes in the chemical unit cell. The diffraction pattern at 295 K is consistent with the calculated pattern above in the same figure. In addition, clear additional diffraction peaks indicated by the arrows are observed at 10 K. By carrying out the low-temperature x-ray diffraction measurements down to 10 K,[29] no crystal structural change has been confirmed. Therefore, these additional peaks in the neutron diffraction profile are attributed to the magnetic scattering, revealing that the β-$Mn_{0.75}Os_{0.25}$ alloy has a long-range magnetic order in which the magnetic unit cell is larger than the chemical unit cell. Although the spin structure is not precisely identified yet due to the complicated profile of the magnetic scattering, the ordered state plausibly has a noncollinear antiferromagnetic structure, in consideration of no spontaneous magnetization.[27] This is the first report, to the best of our knowledge, on the direct confirmation of the long-range ordered magnetic state of β-Mn alloys. Accordingly, the small peak or the inflection point in magnetic susceptibility-temperature curves $\chi(T)$ for several kinds of β-Mn alloys[25–29] can be rationalized as the Néel temperature T_N.

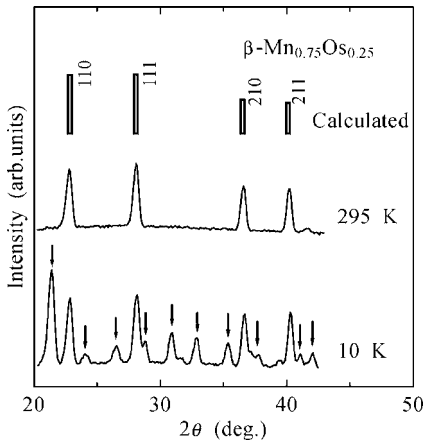

FIG. 1. Powder neutron diffraction patterns of β-$Mn_{0.75}Os_{0.25}$ alloys at 10 and 295 K, together with the calculated pattern of the nuclear contribution above in the same figure.

The concentration dependence of the electronic specific heat coefficient γ of the β-$Mn_{1-x}M_x$ (M=Ru,[25] Os, and Ir) alloys is given in Fig. 2. The value of γ is obtained by a linear extrapolation of the specific heat in the form of C/T versus T^2 (Refs. 25, 27, and 29). The value of γ mainly consists of two terms, the band term γ_{band} and the spin fluc-

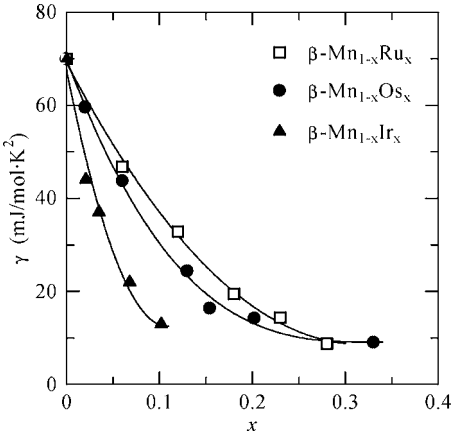

FIG. 2. Concentration dependence of the electronic specific heat coefficient γ of β-$Mn_{1-x}M_x$ [M=Ru, (Ref. 26) Os, and Ir] alloys.

tuation term γ_{sf}. The concentration dependence of γ is significant because the magnitude of γ is influenced by the change in spin-fluctuation features. The contribution of spin fluctuations to the specific heat C_{sf} is given by the following expression.[36]

$$C_{sf} = -T\frac{\partial^2 F_{sf}}{\partial T^2}, \tag{1}$$

with

$$F_{sf} = \sum_q \int_0^\omega d\omega f(\omega)\frac{3}{\pi}\frac{\Gamma_q}{\Gamma_q^2 + \omega^2} \tag{2}$$

and

$$\Gamma_q = \Gamma_0 q(\kappa^2 + q^2), \tag{3}$$

where $f(\omega)$ is the population function of a harmonic oscillator with the frequency ω, and Γ_q is the relaxation frequency of spin fluctuations of the wave vector q. Γ_0 is the spectrum width of spin fluctuations and $1/\kappa$ is the magnetic correlation length. From Eq. (1), the electronic specific heat coefficient enhanced by spin fluctuations, γ_{sf}, is expressed as

$$\gamma_{sf} = \frac{3N_0}{4T_0}\ln\left(1 + \frac{1}{{K_0}^2}\right), \tag{4}$$

where N_0 is the number of the magnetic atom, and T_0 and K_0 are proportional to Γ_0 and κ, respectively. In weak itinerant-electron antiferromagnets, the spin-fluctuation modes with the wave vectors q have strong intensities around the antiferromagnetic vector Q, and hence $1/T_0$ and $1/K_0$ become large. Consequently, γ_{sf} brings about a remarkable contribution to γ. Taking the band term estimated to be 8 mJ/mol K^2 into account,[37] the value of γ_{sf} is extremely large in the low M concentration ranges and rapidly decreases with increasing M concentration, and finally the value of γ becomes close to the value of γ_{band}.[25,27,29]

It has been pointed out that the spin-fluctuation term γ_{sf} of the electronic specific heat coefficient γ is proportional to ${T_N}^{3/4}$ in weak itinerant-electron antiferromagnets.[14] According to the SCR calculation by Hasegawa,[14] γ_{sf} is also expressed by the following expression:

$$\gamma_{sf}(\delta) - \gamma_{band}(\delta) = \gamma_{sf}(1) - \gamma_{band}(1) - W_A(\delta - 1)^{1/2} \tag{5}$$

with

$$\delta = 2I\chi_s, \tag{6}$$

where γ_{band} is the term obtained by the Hartree-Fock approximation, W_A is the constant associated with the band structure, and I and χs are the exchange interaction and the staggered susceptibility, respectively. The magnetic state on the verge of antiferromagnetism is given by $\gamma_{sf}(1)$ and $\gamma_{band}(1)$ in Eq. (5). The value of δ given by Eq. (6) represents the condition of the onset of antiferromagnetism. Depending on the value of δ, that is, below 1 or above 1, the magnetic state becomes paramagnetic or antiferromagnetic, respectively. When the spin-fluctuation modes with the wave vectors q have strong intensities around the antiferromagnetic vector Q, T_N is related to the following relation:[30]

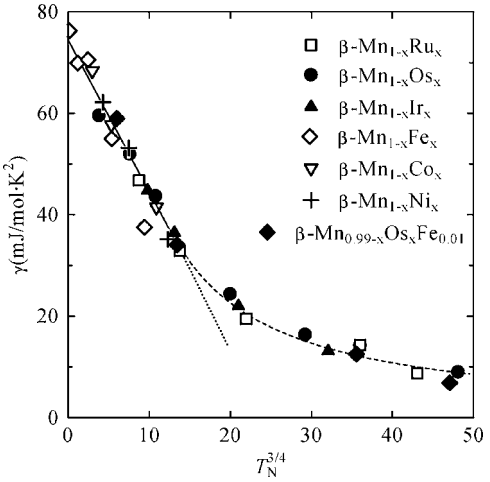

FIG. 3. Relationship between the electronic specific heat coefficient γ and the Néel temperature T_N in the form of γ-${T_N}^{3/4}$ for β-Mn alloys, in which the additional elements preferentially occupy Mn site 1 (Refs. 4, 25, 27, and 29). The dashed line is only to guide the eyes.

$$T_N \propto (\delta - 1)^{2/3}. \tag{7}$$

Therefore, the relation between γ_{sf} and T_N is given by the following expression in weak itinerant-electron antiferromagnets:

$$\gamma_{sf} = A - B{T_N}^{3/4}, \tag{8}$$

where A and B are the constants. Figure 3 shows the relation between the Néel temperature T_N and the electronic specific heat coefficient γ of the β-Mn alloys, in which the additional elements preferentially occupy site 1.[4,25,27,29] The data of the β-$Mn_{0.99-x}Os_xFe_{0.01}$ alloys are included in Fig. 3, which is the sample for Mössbauer spectroscopy as described later in connection with Fig. 12. The plots in the form of γ-${T_N}^{3/4}$ are consistent by assuming that the value of γ_{band} is scarcely sensitive to the kinds of additional elements. The value of γ is proportional to ${T_N}^{3/4}$ in the low M concentrations, and in the range of the high γ values, all the data are plotted on the same straight line without regard to the kinds of the additional elements. However, with increasing additional element concentration, or with increasing T_N, the gradual reduction of γ leads to a relative increase of γ from the straight line, and hence the alloys are no longer weak itinerant-electron antiferromagnets, and eventually γ becomes close to the value of γ_{band}. Therefore, it is concluded that the magnetic state in the β-Mn alloys changes from the weak itinerant-electron antiferromagnetic to the intermediate antiferromagnetic state with increasing additional element concentration.[25,27,29] In the present paper, the intermediate antiferromagnetic state is defined as the magnetic state that deviates from the linear relation of the γ-${T_N}^{3/4}$ plot. Such a change is a characteristic to the β-$Mn_{1-x}M_x$ (M=Ru, Os, and Ir) alloys. The significantly large value of γ in the β-Mn alloys is attributed to the effect of spin fluctuations, which is also reflected to the spontaneous volume magnetostriction below T_N as well as the thermal expansion coefficient above T_N.

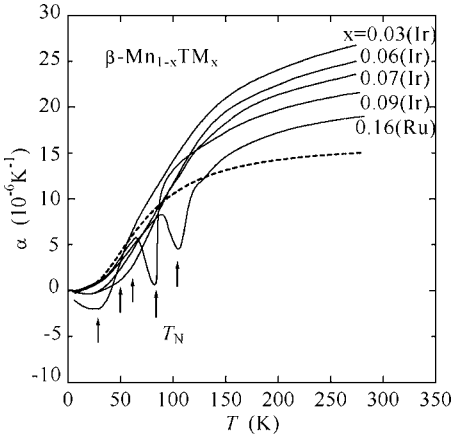

FIG. 4. Temperature dependence of the thermal expansion coefficient α for β-$Mn_{1-x}M_x$ (M=Ru and Ir) alloys. The arrows indicate the Néel temperature T_N determined from the magnetic susceptibility measurement. The solid lines stand for the total thermal expansion curves. The dashed line stands for the lattice term.

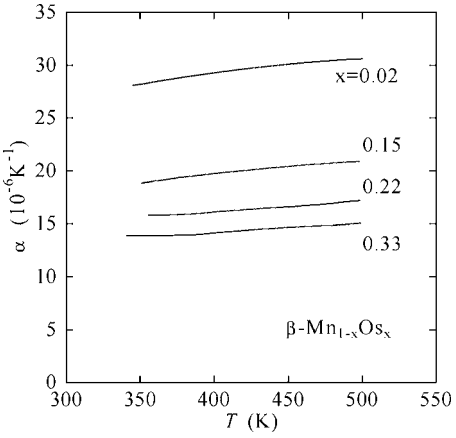

FIG. 5. Temperature dependence of the thermal expansion coefficient α of β-$Mn_{1-x}Os_x$ alloys above the Néel temperature.

Shown in Fig. 4 is the temperature dependence of the thermal expansion coefficient α of the β-$Mn_{1-x}M_x$ (M=Ru and Ir) alloys. The arrows indicate the Néel temperature T_N determined from the temperature dependence of magnetic susceptibility. The thermal expansion coefficient α is given by the following expression:

$$\alpha = \alpha_{lat} + \alpha_{ele} + \alpha_{mag}, \tag{9}$$

where $\alpha_{lat}, \alpha_{ele}$, and α_{mag} are the lattice, electron, and magnetic terms, respectively. It should be noted that the electronic term is about two orders of magnitude smaller than the lattice term,[38] and hence we can regard it as $(\alpha_{lat}+\alpha_{ele}) \sim \alpha_{lat}$. To discuss the magnetic term, we estimate the lattice term from the specific heat data. The thermodynamic relation between the specific heat C and the thermal expansion coefficient α_{lat} is given by

$$\alpha_{lat} = \Gamma k C, \tag{10}$$

where Γ is the Grüneisen constant and k is the compressibility. The value of α_{lat} is proportional to C approximated by the Debye function. The Debye temperature obtained from low-temperature specific heat measurements is about 300 K, almost independent of the additional elements and their concentrations.[29] Therefore, the magnitude of the lattice term is regarded as almost the same in these alloys. The value of γ of the β-$Mn_{1-x}Os_x$ alloys with x=0.33 is close to that of γ_{band}, indicating the effect of spin fluctuations on the thermal expansion is weak and the thermal expansion coefficient of the lattice term is about 15×10^{-6} K^{-1} at room temperature,[28] therefore, the lattice term is given by the dashed line in Fig. 4. As a result, the lattice term exceeds the solid line below T_N, showing a positive spontaneous volume magnetostriction below T_N in all the composition including in low Ir concentration regions, although the previous thermal expansion curves obtained by x-ray diffractions exhibit no clear spontaneous volume magnetostriction because of a low accuracy.[28] Moreover, the pronounced decrease of α at T_N occurs in the alloys having the intermediate antiferromagnetic state. The thermal expansion coefficient above T_N for the β-$Mn_{1-x}M_x$ alloys is larger than that of the lattice term.

According to the unified model based on the SCR theory,[30] for the change from the itinerant-electron magnetism to the localized-electron magnetism, the important factors for magnetic materials are the thermal average of local magnetic moment $\langle M_{Loc}(T)^2\rangle$ and its temperature dependence, which is reflected in the magnetic term $\alpha_{mag} = (1/3)d\omega_{mag}(T)/dT$ of the thermal expansion. Thus, $\langle M_{Loc}(T)^2\rangle$ and $\omega_{mag}(T)$ are, respectively, given by the following expressions:[39,40]

$$\langle M_{Loc}(T)^2\rangle = m(T)^2 + \langle \xi(T)^2\rangle \tag{11}$$

and

$$\omega_{mag}(T) \propto \langle M_{Loc}(T)^2\rangle, \tag{12}$$

where $\langle \xi(T)^2\rangle$ and $m(T)^2$ are, respectively, the mean-square local amplitude of spin fluctuations and the square uniform magnetization, respectively. For itinerant-electron ferromagnets and antiferromagnets, $m(T)^2$ decreases and disappears at the magnetic transition temperature with increasing temperature. On the other hand, $\langle \xi(T)^2\rangle$ increases through the magnetic transition temperature with increasing temperature. For weak itinerant-electron magnets, the temperature dependence of $\langle \xi(T)^2\rangle$ and $d\langle \xi(T)^2\rangle/dT$, is extremely large, and hence the thermal expansion coefficient α in paramagnetic regions exhibits a large value.[30] In Fig. 4, the large room-temperature value of α becomes smaller with increasing x, reflecting the decrease of $\langle \xi(T)^2\rangle$ and $d\langle \xi(T)^2\rangle/dT$. Figure 5 shows the temperature dependence of the thermal expansion coefficient α above the Néel temperature T_N for the β-$Mn_{1-x}Os_x$ alloys. The value of α increases with increasing temperature in the wide range of temperature above T_N for all the composition. The value of α above x=0.22 becomes smaller with increasing x and weakly depends on x as seen from Fig. 5. That is, it is characteristic of the thermal expansion properties in the β-Mn alloy system that both of $\langle \xi(T)^2\rangle$ and $d\langle \xi(T)^2\rangle/dT$ decrease with increasing x, especially in the range of low x. The thermal expansion coefficient in paramagnetic regions

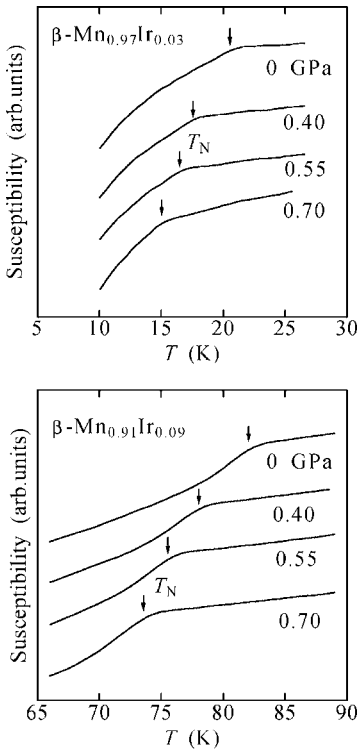

FIG. 6. Temperature dependence of the magnetic susceptibility under pressure of β-$Mn_{1-x}Ir_x$ alloys. The arrows indicate the Néel temperature T_N.

will be discussed again in connection with the electronic specific heat coefficient data in Fig. 11.

It is well known that the thermal expansion properties are thermodynamically correlated to the pressure dependence of the Néel temperature T_N. In the second-order transition, the Ehrenfest equation is given by

$$\frac{dT_N}{dP} = VT_N\frac{\Delta\alpha_V}{\Delta C_m}, \tag{13}$$

where $V, \Delta\alpha_V$, and ΔC_m are the volume, the difference between the volume thermal expansion coefficient below and above T_N, and also the difference between the specific heat, respectively. In the β-Mn alloys, $\Delta\alpha_V$ is negative and ΔC_m is positive and, accordingly, dT_N/dP is expected to be negative.[28]

Shown in Fig. 6 is the temperature dependence of magnetic susceptibility under pressure for the β-$Mn_{1-x}Ir_x$ alloys. The arrows indicate the Néel temperature T_N. Such negative pressure dependence of T_N is observed in all the specimens with different compositions. We have used a piston-cylinder cell made of a Cu-Ti alloy, which enables us to measure the magnetic susceptibility with a high sensitivity[35] because the magnetic susceptibility of the β-$Mn_{1-x}M_x$ (M=Ru, Os, and Ir) alloys is small and its temperature dependence is very weak.[25–29] The pressure dependence of the Néel temperature T_N for the β-$Mn_{1-x}Ru_x$ (a), β-$Mn_{1-x}Os_x$ (b),[28] and β-$Mn_{1-x}Ir_x$ (c) is given in Fig. 7. Only the pressure dependence of T_N for the β-$Mn_{1-x}Os_x$ alloys (x=0.14, 0.17, 0.22, and 0.33) obtained by the electrical resistivity measurement

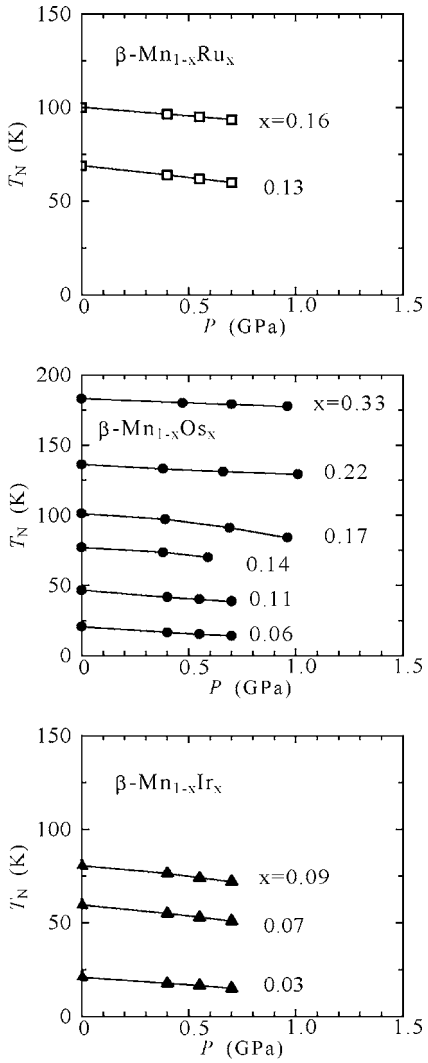

FIG. 7. Pressure dependence of the Néel temperature T_N for (a) β-$Mn_{1-x}Ru_x$, (b) β-$Mn_{1-x}Os_x$ (Ref. 28), and (c) β-$Mn_{1-x}Ir_x$ alloys.

has been reported previously, and the minimum of the temperature derivative in the electrical resistivity corresponds to the Néel temperature determined from magnetic measurements.[28] The value of T_N decreases linearly under 1 GPa, and the pressure dependence of T_N is almost the same. Figure 8 shows the relationship between the pressure dependence of the Néel temperature dT_N/dP and T_N for the β-$Mn_{1-x}M_x$ (M=Ru, Os, and Ir) alloys. A broad maximum is observed around T_N=70 K. It is interesting to note that the β-Mn alloys with around T_N=70 K change their magnetic state from the weak itinerant-electron antiferromagnetic to the intermediate antiferromagnetic state as seen from Fig. 3. The value of dT_N/dP is proportional to the volume change at T_N as given by Eq. (13), consequently, the broad maximum in Fig. 8 is reflected to the magnitude of the spontaneous volume magnetostriction at T_N. In the alloys with the lower Néel temperature, although the volume change is hardly observed, dT_N/dP is not so small, implying that the contribution from ΔC_m is dominant. The temperature dependence of the specific heat of the β-$Mn_{1-x}Ir_x$ alloys is illustrated in Fig. 9. The arrows in the figure indicate the Néel temperature T_N

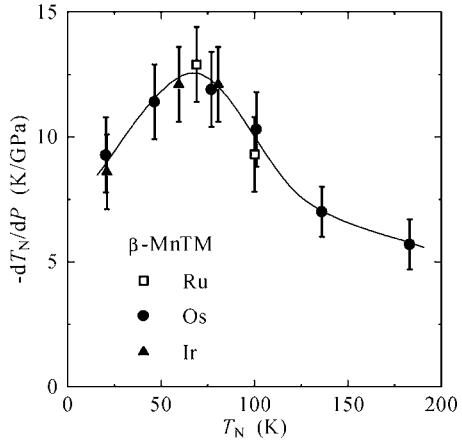

FIG. 8. Relationship between the pressure dependence of the Néel temperature dT_N/dP and T_N of β-$Mn_{1-x}M_x$ (M=Ru, Os, and Ir) alloys.

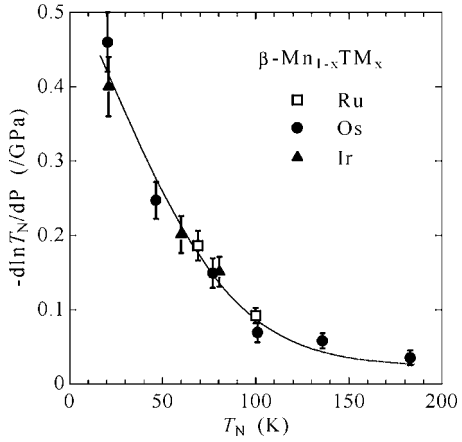

FIG. 10. Concentration dependence of the pressure coefficient of the Néel temperature T_N for β-$Mn_{1-x}M_x$ [M=Ru, Os (Ref. 28), and Ir] alloys.

obtained from the temperature dependence of magnetic susceptibility. No clear peak is observable at T_N and a very broad anomaly is observed around T_N with increasing x, and finally a distinct peak is observed at x=0.09. In β-MnFe, β-MnCo, and β-MnNi alloys, the peak at T_N is hardly observed from the specific heat measurements.[4] In weak itinerant-electron antiferromagnets, the spin-fluctuation modes with the wave vectors q have strong intensities around the antiferromagnetic vector Q and also the magnetic correlation length $1/\kappa$ becomes significantly large, diverging at the Néel temperature T_N. The peak around T_N becomes smaller with decreasing x, suggesting that the spin-fluctuation modes around Q are excited in a wider temperature range around T_N with decreasing x. According to the spin-fluctuation theory including the quantum spin fluctuations, weak itinerant-electron magnets hardly exhibit a clear magnetic entropy peak at T_N.[41,42] Similar behavior has been observed in the β-$Mn_{1-x}Ru_x$ and β-$Mn_{1-x}Os_x$ alloys.[25,27] As described above, the magnetic correlation length is large and ΔC_m is very small in the alloys with the low Néel temperature. Consequently, dT_N/dP is relatively large, in spite of a small value of $\Delta\alpha_V$.

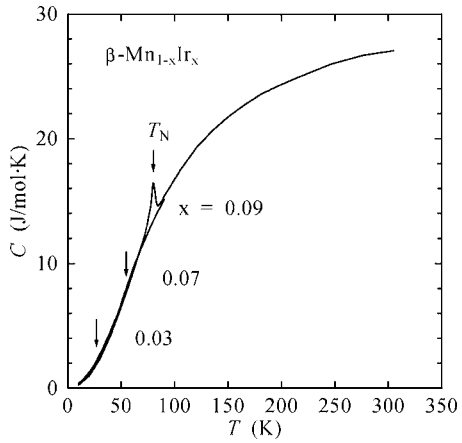

FIG. 9. Temperature dependence of the specific heat of β-$Mn_{1-x}Ir_x$ alloys. The arrows indicate the Néel temperature T_N determined from the temperature dependence of magnetic susceptibility.

The pressure coefficient of the β-$Mn_{1-x}M_x$ (M=Ru, Os,[28] and Ir) alloys is plotted against the Néel temperature T_N in Fig. 10. The magnitude of the pressure coefficient drastically decreases with increasing T_N. Generally, the pressure coefficient of weak itinerant-electron magnets is large. For example, the pressure coefficient of the Curie temperature is -0.11 GPa^{-1} for Ni_3Al,[43] -0.39 GPa^{-1} for MnSi,[44] and 0.33 GPa^{-1} for Sc_3In.[45] In lower concentration regions, the pressure coefficient is almost the same as that of weak itinerant-electron magnets, furthermore, the pressure coefficient is still relatively large in higher concentration regions, because these alloys are not in a complete localized-electron antiferromagnetic state but in an intermediate antiferromagnetic state. It is clear that the variation of the pressure coefficient with increasing x in the β-$Mn_{1-x}M_x$ (M=Ru, Os,[28] and Ir) alloys reflects the change in the magnetic state from the weak itinerant-electron antiferromagnetic state to the intermediate state.

The effect of spin fluctuations at low temperatures is reflected in the electronic specific heat coefficient as given in Fig. 3. On the other hand, the thermal expansion coefficient in the paramagnetic state is also affected by the spin fluctuations at finite temperatures. In order to discuss the effect of $\langle\xi(T)^2\rangle$ on the thermal expansion, α_{mag} is normalized to enough high paramagnetic temperature, $3T_N$, and plotted against T_N in Fig. 11 for the β-$Mn_{1-x}M_x$ (M=Ru, Os, and Ir). In the figure, the solid and dashed lines are guides to the eye. Similar to the electronic specific heat coefficient affected by the spin fluctuations at low temperatures, the thermal expansion coefficient at finite temperatures decreases with increasing T_N or x. Accordingly, it is concluded from Figs. 3 and 11 that the effects of spin fluctuations at low and finite temperatures in both the magnetic states are observed without regard to the kinds of substituted elements in the β-Mn alloys. In itinerant-electron magnets, the spin fluctuations can be characterized by two terms in Eq. (4); T_0, which corresponds to the energy scale of spin fluctuations, and $1/K_0$, which is proportional to the magnetic correlation length. In weak

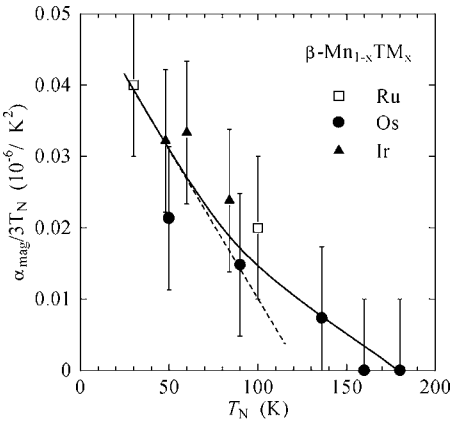

FIG. 11. Relationship between the magnetic term of the thermal expansion coefficient at $3T_N$, $\alpha_{mag}(3T_N)$, in the form of $\alpha_{mag}(3T_N)/3T_N$ and the Néel temperature T_N of β-$Mn_{1-x}M_x$ (M=Ru, Os, and Ir) alloys. The solid and dashed lines are only guides to the eyes.

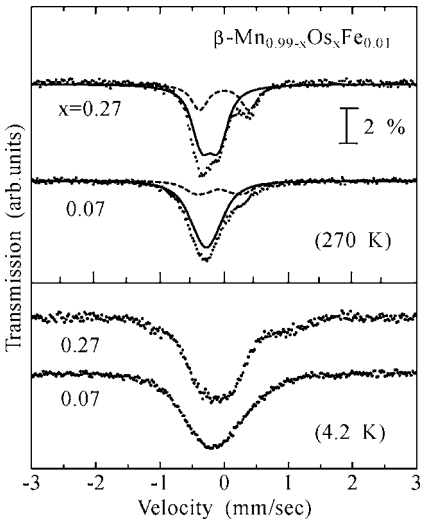

FIG. 12. Mössbauer spectra of β-$Mn_{0.99-x}Os_xFe_{0.01}$ alloys at 4.2 and 270 K. The solid and dashed lines represent the contributions from Mn sites 1 and 2, respectively.

itinerant-electron magnets, both the values of $1/T_0$ and $1/K_0$ are large in analogy with pure β-Mn metal.[30] Adding Ru, Os, and Ir to β-Mn, both the values of $1/T_0$ and $1/K_0$ drastically decrease, approaching to the intermediate state. From Figs. 3 and 11, the rate of decrease of $1/T_0$ and $1/K_0$ would be almost the same against the Néel temperature T_N in the β-$Mn_{1-x}M_x$ (M=Ru, Os, and Ir) alloys. Moreover, in the β-MnFe alloy, it has been pointed out from the Mössbauer spectroscopy that Fe atoms have no localized moment;[46] therefore, it is considered that the addition of Fe atoms is the same as the addition of a nonmagnetic atom such as Ru, Os, and Ir; therefore, the effect of spin fluctuations is considered to be almost the same, regardless of additional elements which preferentially occupy Mn site 1.

From the temperature dependence of spin lattice relaxation rate $1/T_1$ of β-Mn, it is expected that the magnetic contribution from two kinds of Mn sites in the β-$Mn_{1-x}M_x$ alloys would be much different to each other. Therefore, we investigate the Mössbauer effects in the β-$Mn_{0.99-x}Os_xFe_{0.01}$ alloys. The Mössbauer spectra of the β-$Mn_{0.99-x}Os_xFe_{0.01}$ alloys at 270 K and 4.2 K are given in Fig. 12. The Mössbauer spectra corresponding to two inequivalent Mn sites are observed in the paramagnetic state spectra at 270 K; the solid and dashed lines stand for the contributions of Mn sites 1 and 2, respectively. The quadrupole shift (QS) of the atomic sites 1 and 2 for the β-$Mn_{0.99-x}Os_xFe_{0.01}$ alloys at 270 K is listed in Table I. The quadrupole shift of atomic site 2 is several times larger than that of atomic site 1, and both the values of the QS increase with increasing x. The broadening of the spectra of each Mn sites at 4.2 K is attributed to the magnetic hyperfine field below T_N, indicating that each Mn site is more or less responsible for the magnetic properties of β-Mn alloys. Very recently, Mn_3IrSi has been reported to have an ordered β-Mn structure, showing a complex noncollinear magnetic structure with magnetic moments of $2.97\mu_B$ at 10 K.[47] The crystal structure of Mn_3IrSi is found to be of the $AlAu_4$ type, with the space group $P2_13$, Mn in a 12b site and Ir and Si in two separate 4a sites, that corresponds to an ordered β-Mn type, the space group $P4_132$, the 8c site of β-Mn is split into two atomic sites. The powder neutron diffraction pattern of Mn_3IrSi includes the magnetic peak of only Mn site 2 in β-Mn structure. On the other hand, for the Mössbauer effects in the β-$Mn_{0.99-x}Os_xFe_{0.01}$ alloys, the magnetic contribution from both Mn sites 1 and 2 is included. The hyperfine field of Mn site 1 in Fig. 12 hardly depends on the composition, whereas that of Mn site 2 increases with increasing x. Namely, the magnetic contribution from Mn site 2 in the β-$Mn_{0.99-x}Os_xFe_{0.01}$ alloys becomes stronger as it approaches the intermediate state. Similar results were obtained from the NMR study of the β-$Mn_{1-x}Os_x$ alloy.[48] It has been reported from the NMR study that the static Mn moment at Mn site 2 increases from $0.3\mu_B$ at x=0.01 to $0.9\mu_B$ at x=0.22 with increasing x or T_N for the β-$Mn_{1-x}Os_x$ alloy.[48] The relatively large static moment with a low T_N would be connected with large spin fluctuations in analogy with a pure β-Mn. It has been reported that the amplitudes of dynamical Mn moments from neutron scatterings at 7 K and 290 K for pure β-Mn obtained are about $1.0\mu_B$ and $1.5\mu_B$ respectively.[16] As mentioned before in connection with Figs. 3 and 11, the effects of spin fluctuations in the β-$Mn_{1-x}M_x$ (M=Ru, Os, and Ir) alloys reduce with increasing x, especially in the range of low x. Additionally, when the spin-fluctuation modes with the wave vectors q have strong intensities around the antiferromagnetic vector Q, i.e., weak itinerant-electron antiferromagnets that belong to the limit of itinerant-electron mangets, the value of γ is proportional to $T_N^{3/4}$ and the peak at T_N is hardly

TABLE I. Quadrupole shift (Q. S.) at 270 K at Mn sites 1 and 2 for β-$Mn_{0.99-x}Os_xFe_{0.01}$ alloys.

	QS (site 1) (mm/s)	QS (site 2) (mm/s)
β-$Mn_{0.92}Os_{0.07}Fe_{0.01}$	0.24_2	0.65_1
β-$Mn_{0.72}Os_{0.27}Fe_{0.01}$	0.27_0	0.77_3

observed in the specific heat curve. With increasing concentration of the additional element, the relation of γ-$T_N^{3/4}$ is not satisfied and the peak at T_N is clearly observed in the specific heat curve. Consequently, the magnetic state changes into the intermediate state, which is very close to weak itinerant-electron antiferromagnets, as compared with localized-electron antiferromagnets. In addition, the static moment drastically increases with increasing additional element concentration, and its value becomes about $1.0\mu_B$ or more in the intermediate antiferromagnetic state in the β-$Mn_{1-x}M_x$ (M=Ru, Os, and Ir) alloys. What has to be mentioned is that the experimental value of γ for the β-$Mn_{0.75}Os_{0.25}$ alloy having the long-range antiferromagnetic order is close to γ_{band} as discussed in connection with Fig. 3. Furthermore, the spontaneous volume magnetostriction for β-$Mn_{0.83}Ru_{0.17}$ and β-$Mn_{0.91}Ir_{0.01}$ in Fig. 4 is explained by the thermal variation of amplitude of local magnetic moment. Consequently, in the concentration region where the γ-$T_N^{3/4}$ relation is not satisfied, the magnetic properties are still dominated by the itinerant character of Mn 3*d* electrons, and thermal fluctuations of amplitude of local moment remain, although the spectral width in the Eq. (2) is wider, compared with that in the region where the γ-$T_N^{3/4}$ relation is valid. From Fig. 12, the continuous increase of the internal field at Mn site 2 with increasing x is clearly observed in the β-$Mn_{1-x}Os_x$ alloy, indicating the itinerant-electron antiferromagnetic properties.[48] Accordingly, it is considered that the continuous increase of the internal field at Mn site 2 is closely connected with the formation of the long-range antiferromagnetic order in the β-$Mn_{1-x}Os_x$ alloy. Note that the internal field at Mn site 2 is almost saturated with increasing x in the β-$Mn_{1-x}Al_x$ alloy in which the additional elements almost mainly occupy Mn site 2.

IV. CONCLUSION

In order to discuss contributions from spin fluctuations in the β-$Mn_{1-x}M_x$ (M=Ru, Os, and Ir) alloys, the thermal expansion and specific heat under ambient pressure and the temperature dependence of the magnetic susceptibility under high pressures have been investigated. The powder neutron diffraction experiment has been performed in order to confirm directly the magnetic state. In connection with the change in the magnetic state, the thermal expansion coefficient above the Néel temperature T_N and the effect of pressure on T_N have been discussed in terms of the spin fluctuations. The main results are summarized as follows.

(1) A long-range magnetic order has been confirmed by neutron powder diffractions for β-$Mn_{0.75}Os_{0.25}$ alloys, supporting that the peak or inflection point in the susceptibility curves of β-$Mn_{1-x}M_x$ alloys corresponds to the Néel temperature.

(2) The dT_N/dP vs T_N plots for β-$Mn_{1-x}M_x$ alloys are given by a universal curve, showing a broad maximum around at 70 K.

(3) A significantly large thermal expansion coefficient in a wide range of temperature above T_N is closely correlated with spin fluctuations.

(4) At low and finite temperatures, the effects of spin fluctuations as a function of T_N in both the weak itinerant-electron and intermediate antiferromagnetic states are almost the same, without regard to the kinds of additional elements.

ACKNOWLEDGMENTS

M. M. is grateful to the support of the JSPS Research Foundation. We gratefully acknowledge Professor K. Ohoyama and K. Nemoto of Institute for Materials Research, Tohoku University for their support of the neutron scattering measurements and useful discussion. A part of the present study was carried at the Laboratory for Advanced Materials, Institute for Materials Research, Tohoku University.

[1] Y. Kohori, Y. Noguchi, and T. Kohara, J. Phys. Soc. Jpn. **62**, 447 (1993).
[2] J. S. Kasper and B. W. Roberts, Phys. Rev. **101**, 537 (1956).
[3] Y. Masuda, K. Asayama, S. Kobayashi, and J. Itoh, J. Phys. Soc. Jpn. **19**, 460 (1964).
[4] T. Shinkoda, K. Kumagai, and K. Asayama, J. Phys. Soc. Jpn. **46**, 1754 (1979).
[5] G. L. Booth, F. E. Hoare, and B. T. Murphy, Proc. Phys. Soc. London, Sect. B **68B**, 830 (1955).
[6] S. Akimoto, T. Kohara, and K. Asayama, Solid State Commun. **16**, 1227 (1975).
[7] M. Katayama, S. Akimoto, and K. Asayama, J. Phys. Soc. Jpn. **42**, 97 (1977).
[8] G. D. Preston, Philos. Mag. **5**, 1207 (1928).
[9] M. O'Keefe and S. Anderson, Acta Crystallogr., Sect. A: Cryst. Phys., Diffr., Theor. Gen. Crystallogr. **33**, 914 (1977).
[10] U. El-Hannany and W. W. Warren, Phys. Rev. B **12**, 861 (1975).
[11] H. Oyamatsu, Y. Nakai, and N. Kunitomi, J. Phys. Soc. Jpn. **58**, 3606 (1989).
[12] T. Kohara and K. Asayama, J. Phys. Soc. Jpn. **37**, 401 (1974).
[13] M. Katayama and K. Asayama, J. Phys. Soc. Jpn. **44**, 425 (1978).
[14] H. Hasegawa, J. Phys. Soc. Jpn. **38**, 107 (1975).
[15] Y. Kohori, Y. Iwamoto, K. Uemura, Y. Akimoto, and T. Kohara, Physica B **223–224**, 594 (1996).
[16] H. Nakamura, K. Yoshimura, M. Shiga, M. Nishi, and K. Kakurai, J. Phys.: Condens. Matter **9**, 4701 (1997).
[17] H. Nakamura and M. Shiga, Physica B **237/238**, 453 (1997).
[18] J. R. Stewart, A. D. Hillier, S. H. Kilcoyne, P. Manuel, M. T. F. Telling, and R. Cywinski, J. Magn. Magn. Mater. **177–181**, 602 (1998).
[19] J. R. Stewart and R. Cywinski, Phys. Rev. B **59**, 4305 (1999).
[20] M. Mekata, H. Nakamura, M. Shiga, G. M. Luke, K. M. Kojima, B. Nachumi, M. Larkin, Y. Fudamato, and Y. J. Uemura, Hyperfine Interact. **120/121**, 639 (1999).
[21] V. Sliwko, P. Mohn, and K. Schwarz, J. Phys.: Condens. Matter **6**, 6557 (1994).

[22] T. Asada, J. Magn. Magn. Mater. **140–144**, 47 (1995).
[23] B. Canals and C. Lacroix, Phys. Rev. B **61**, 11251 (2000).
[24] J. Hafner and D. Hobbs, Phys. Rev. B **68**, 014408 (2003).
[25] K. Sasao, R. Y. Umetsu, and K. Fukamichi, J. Alloys Compd. **325**, 24 (2001).
[26] R. Yamauchi, M. Miyakawa, K. Sasao, and K. Fukamichi, J. Alloys Compd. **311**, 124 (2000).
[27] M. Miyakawa, R. Y. Umetsu, and K. Fukamichi, J. Phys.: Condens. Matter **13**, 3809 (2001).
[28] M. Miyakawa, R. Y. Umetsu, K. Fukamichi, H. Yoshida, and E. Matsubara, J. Phys.: Condens. Matter **15**, 4817 (2003).
[29] M. Miyakawa, R. Y. Umetsu, K. Sasao, and K. Fukamichi, J. Phys.: Condens. Matter **15**, 4605 (2003).
[30] T. Moriya, *Spin Fluctuation in Itinerant Electron Magnetism* (Springer, Berlin, 1985).
[31] S. Funahashi and T. Kohara, J. Appl. Phys. **55**, 2048 (1984).
[32] T. Hori, J. Phys. Soc. Jpn. **38**, 1780 (1975).
[33] J. R. Stewart and R. Cywinski, J. Magn. Magn. Mater. **272–276**, 676 (2004).
[34] K. Ohoyama, T. Kanouchi, K. Nemoto, M. Ohashi, T. Kajitani, and Y. Yamaguchi, Jpn. J. Appl. Phys., Part 1 **37**, 3319 (1998).
[35] K. Koyama, S. Hane, K. Kamishima, and T. Goto, Rev. Sci. Instrum. **69**, 3009 (1998).
[36] R. Konno and T. Moriya, J. Phys. Soc. Jpn. **56**, 3270 (1987).
[37] N. Mori, T. Ukai, K. Sasaki, and P. Rhoden, *Physics of Transition Metals, Institute of Physics Conference Series* (Institute of Physics, Bristol, 1980), Vol. 55, p. 21.
[38] S. Ogawa, Physica B **119**, 68 (1983).
[39] T. Moriya and K. Usami, Solid State Commun. **34**, 95 (1980).
[40] H. Yamada and K. Terao, J. Phys.: Condens. Matter **6**, 10805 (1994).
[41] Y. Takahashi, J. Phys.: Condens. Matter **11**, 6439 (1999).
[42] Y. Takahashi and H. Nakano, J. Phys.: Condens. Matter **16**, 4505 (2004).
[43] N. Buis, J. M. Franse, and P. E. Brommer, Physica B **106**, 1 (1981).
[44] D. Bloch, J. Voiron, J. Jaccarino, and J. H. Wernick, Phys. Lett. **51A**, 259 (1975).
[45] J. Grewe, J. S. Schilling, K. Ikeda, and K. A. Gschneidner Jr., Phys. Rev. B **40**, 9017 (1989).
[46] Y. Nishihara, S. Ogawa, and S. Waki, J. Phys. Soc. Jpn. **42**, 845 (1977).
[47] T. Eriksson, R. Lizarraga, S. Felton, L. Bergqvist, Y. Andersson, P. Nordblad, and O. Eriksson, Phys. Rev. B **69**, 054422 (2004).
[48] T. Hama, M. Matsumura, H. Yamagata, M. Miyakawa, R. Y. Umetsu, and K. Fukamichi, J. Magn. Magn. Mater. **272–276**, 503 (2004).